Tree-ring growth and hydro-climatic variability in temperate dendrochronologies of northern Mexico

Crecimiento de anillos y variabilidad hidro-climática en dendrocronologías templadas del norte de México

José Návar[1] and Liliana Lizárraga-Mendiola[2]

ABSTRACT

This report addresses the following questions: a) is the diameter growth described by the standard ring width anomaly (SRWA) of *Psudotsuga menziesii* (Mirb.) Franco trees related to precipitation (P), pan evaporation (E), evapotranspiration (Et), runoff (Q), and soil moisture content (θ) derived from a water balance model?; b) is the SRWA associated with synoptic climate events such as El Niño Southern Oscillation (ENSO), the Pacific Decadal Oscillation (PDO), and the Atlantic Multidecadal Oscillation (AMO)?, and c) are P, Et and θ related to ENSO, PDO and AMO events? The SRWA for three dendrochronologies (Las Bayas and Banderas in Durango and El Gato in Zacatecas) from 1665 to 2001 addressed these questions. Instrumental measurements of P and E (1947-2007) and, using parameterized sub-models for the rainfall interception of Gash model (I) and Et, a mass balance approach evaluated Q and θ for a forest site near El Salto, Durango, Mexico. SRWA oscillations of several timescales had spectral peaks every 2-3; 3-7; and 9-12 years. The ENSO indices explained most of the total SRWA variation for all three chronologies (1990-2001). For the short (1990-2001) and middle-term (1945-2001) seasonal data, the SRWA variability was only linked to θ. The strength of the relationship weakened as the length of the time series increased, indicating that other variables control tree growth as well. The ENSO takes, on average, 4 to 8 months to display its effect on the hydrological variables and diameter growth in northern *P. mensiezii* trees of Mexico, making tree growth predictable.

Key words: mensuration, climate change, bioclimatic indexes, El Niño-Southern Oscillation, Pacific Decadal Oscillation, Atlantic Multidecadal Oscillation.

RESUMEN

Este reporte plantea las siguientes preguntas: a) se encuentra el crecimiento diamétrico descrito por la anomalía de la amplitud del anillo de crecimiento estándar (SRWA) de árboles de *Pseudotsuga menziesii* (Mirb.) Franco relacionado con la precipitación (P), la evaporación (E), la evapotranspiración (Et), el escurrimiento (Q) y el contenido de humedad del suelo (θ), derivados de un modelo del balance hidrológico?; b) se encuentra el SRWA asociado con eventos climáticos sinópticos tales como El Niño-Oscilación del Sur (ENSO), la Oscilación Decadal del Pacífico (PDO), y la Oscilación Multidecadal del Atlántico (AMO)? y c) se encuentran P, Et y θ relacionados con ENSO, PDO y AMO? Los datos de SRWA para tres cronologías (Las Bayas y Banderas en Durango, y El Gato en Zacatecas) de 1665 hasta 2001 sirvieron para resolver estas preguntas. Mediciones instrumentales de P y E (1947-2007) y con el uso de sub-models paramétricos para la intercepción de la lluvia del modelo Gash (I) y Et, el procedimiento del balance de masas evaluó Q y θ para una cuenca cerca de El Salto, Durango, México. Oscilaciones de SRWA de varias escalas de tiempo mostraron picos espectrales cada 2-3; 3-7; y 9-12 años. Los índices de ENSO explicaron parte de la variación de SRWA para las tres cronologías (1990-2001). Para datos estacionales (1990-2001) y de escala mediana (1845-2001) θ explicó mejor la variación de SRWA. La fortaleza de la relación se debilita con la longitud de la serie de tiempo indicando otras variables controlan el crecimiento. El ENSO toma en promedio de 4 a 8 meses para mostrar su efecto en las variables hidrológicas locales y en el crecimiento diamétrico de árboles de *P. menziesii* del norte de México haciendo el crecimiento forestal predecible en el tiempo.

Palabras clave: mediciones forestales, cambio climático, índices bioclimáticos, El Niño Oscilación del Sur, Oscilación Decadal del Pacífico, Oscilación Multidecedal del Atlántico.

Introduction

Assuming factors that control tree growth (*e.g.*, soil fertility and atmospheric carbon) are constant over time and removing age-related growth patterns, tree growth deviations must be partially dependent on climatic variability (Sathle *et al*., 1999). In northern Mexico, precipitation and temperature are spatially and temporally modified by large-scale synoptic climatic events (Cavazos and Hastenrath,

Received for publication: 18 December, 2013. Accepted for publication: 19 March, 2014.

[1] Centro del Agua para América Latina y El Caribe, Instituto Tecnológico y de Estudios Superiores de Monterrey (ITESM). Monterrey (Mexico). jnavar@itesm.mx

[2] Environmental Engineering, Universidad Autónoma del Estado de Hidalgo. Mineral de la Reforma (Mexico).

1990; Comrie and Glenn, 1998) and might control tree growth as well.

Climatic variability has been linked to tree growth in many places (Fritts, 1976; Briffa, 2000; Fang *et al*., 2012). Climate-growth relationships are more evident in places with large scale latitudinal and longitudinal gradients (Cook *et al*., 2001; Fang *et al*., 2012). Northern Mexico is located in between the subtropical and the Inter-tropical Convergence Zone circulation regimes, the fundamental reason for the region´s climatic variability (Sheppard *et al*., 2002). In this region, forest growth and hydro-climatic variability have rarely been associated (Cleaveland *et al*., 2003). Climate varies over different timescales (seasonal, inter-annual, 3-7 years; 9-12; 70-80 years) in Little Ice Ages and inter glacial periods, among others (Comrie and Glenn, 1998; Sheppard *et al*., 2002; Návar-Cháidez, 2012; Návar, 2014).

The El Niño Southern Oscillation (ENSO) peaks every 3-7 years and correlates well with tree growth since it causes severe and prolonged summer droughts and cold-wet winters in northern Mexico (González-Elizondo *et al*., 2005), with a reduced total annual rainfall (Cleaveland *et al*., 2003). It has also been correlated to tree growth in many other places (Swetnam and Betancourt, 1998; Briffa, 2000; Worbes, 2002).

The Pacific Decadal Oscillation (PDO) cooling - warming anomaly, a quasi decadal cycle, appears to be related to drought-wet spells in northern Mexico (Jones, 2003). The cooling of the northeastern Pacific Ocean has been linked to above average rainfall and discharge in northern Mexico (Návar-Cháidez, 2012). Its control is not consistent over time and appears insignificant during periods of instrumental recorded data (Tingstad and MacDonald, 2010). Weak associations between hydro-climatic variability and PDO can be explained by the fact that the latter manifests mostly in the North Pacific region and can persist over several decades. Mantua *et al*. (1997) described periods of 15-25 years and 50-70 years and dry spells lasting, at the most, 15 years (1950's) for this time series data.

The AMO oscillation is an Atlantic Ocean sea surface temperature anomaly and returns every 65-80 years, causing worldwide hydro-climatic variability (Knight *et al*., 2006). Positive AMO index values have been related to droughts in the continental US during the 20th Century (Enfield *et al*., 2001). This cycle appears to be linked to hydro-climates as well as to tree growth in northwestern forests of Mexico and elsewhere (Briffa, 2000; Linderholm *et al*., 2003; Návar-Cháidez, 2012).

However, little research has been carried out to determine the climatic variability effect on tree growth in northern, temperate forests of Mexico in order to assess impacts on past, present and future forest productivity. Therefore, this report aimed: a) to statistically correlate precipitation (P), evapotranspiration (Et), and soil moisture content (θ) to ring width anomalies; b) to relate the synoptic-scale climate events Southern Oscillation Index (SOI), ENSO, PDO and AMO to standard ring width anomaly (SRWA); and c) to relate P, Et and θ to ENSO, PDO and AMO events. The hypothesis tested was that SRWA is unrelated to hydro-climatic variability.

Materials and methods

Location of the study area

The study was carried out in the State of Durango, located in the north-central portion of Mexico. It covers an area of 12.3 Mha (Fig. 1) and spans 22°35' N and 104°50' W; 24°44' N and 22°58' W; 26°83' N and 104°27' W, and 23°52' N and 107°21' W. Durango neighbors the States of Chihuahua and Coahuila to the north and to the east; Coahuila and Zacatecas to the east, Zacatecas and Nayarit to the south and Sinaloa and Nayarit to the west. Physiographic regions that characterize the State are; a) the western Plains of the Pacific Ocean, b) the Sierra Madre Occidental mountain range, c) the central valleys of Durango and Chihuahua, and d) the Chihuahuan Desert. The study was conducted in the Sierra Madre Occidental mountain range, SMW.

The SMW ranges from the northwestern to the central portions of the country and serves as the continental and climatic divide. It features several microclimates, according to the Köppen climatic classification scheme as modified for Mexico by García (1987): a) in the highlands, the temperate-cold, humid climate has summer rains and mean annual temperatures between 5 and 12°C. The interior lower ridges are characterized by semi-arid, dry temperate forests with mean annual temperatures ranging from 12 to 18°C. The Pacific Ocean slopes are characterized by dry, warmer climates.

The principal, distributed pine species in the SMW are *Pinus cooperi*, *P. durangensis, P. engelmannii, P. teocote, P. herrerae, P. leiophylla* and *P. ayacahuite*. *Quercus sideroxyla*, *Q. durifolia, Q. rugosa* and *Q. candicans* are the most frequent oak species observed. *Juniperus* sp., *Cupressus* sp., *Pseudotsuga* sp. and *Abies* sp. are other temperate

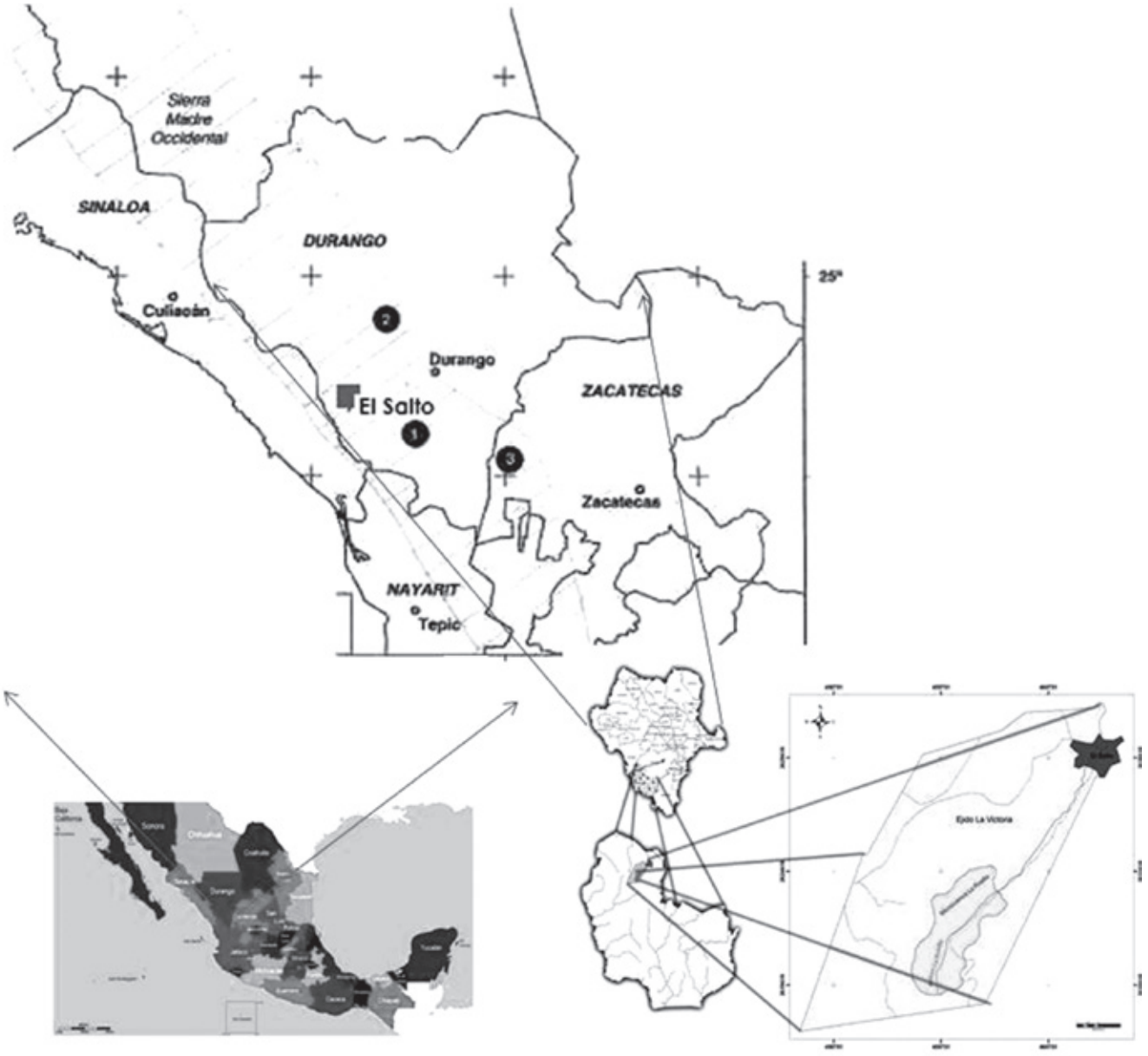

FIGURE 1. Location of the State of Durango in México and the place where wood cores were collected for ring width analysis: (1) Las Bayas; (2) Banderas; (3) El Gato, the climatic station and La Rosilla watershed at El Salto, Durango, Mexico.

conifer species that make up the forest community within the watershed. Other broad leaf species found within these forests are *Arbutus* sp. and *Alnus* sp.

The water balance of forest soils

A model, based on the mass balance budget, physically computed changes in θ as the difference between inputs and outputs. Daily P and pan evaporation (E) measured (1945-2007) variables were collected from Education Resources Information Center-ERIC. Evaluated output variables using models were: interception loss, I, and evapotranspiration (Et= transpiration and evaporation of water from the soil). Assessments of I, runoff (Q), and θ were conducted by fitting the reformulated analytical model of Gash (Gash *et al*., 1995; Valente *et al*., 1997), by making several assumptions for discharge and by running the physical model, respectively; see Eq. 1, 2, 3, 4, and 5.

$$E - S = \frac{\partial A}{\partial t};\ E = P \tag{1}$$

$$S = (I + Ev + Tr + Qs + Qp);\ Et = (Ev + Tr) \tag{2}$$

$$P-(I+Et+Qs+Qp)=\frac{\partial A}{\partial t} \quad (3)$$

$$Q=Qs+Qp; \quad (4)$$

$$Q=P-(I+Et)\pm\frac{\partial A}{\partial t} \quad (5)$$

Q is the excess soil water (*e.g.*, θi ≥ θfc; i = current, fc = field capacity) since no discharge measurements are available at this time for the La Rosilla watershed. The model assumes that above field capacity θ leaks down into shallow water tables that eventually transform into Q via the subsurface, saturated through-flow, and aquifer discharge. High final infiltration rates of the order of 130 mm h^{-1} had been measured and only 7% of the rains occurring annually and close to 30% of the rains with a 2 year return frequency produce Hortonian surface runoff in northern forest watersheds of Mexico (Dueñez-Alanís *et al*., 2006). Then, leakage or percolation estimates, Qs, = discharge, Q, since surface runoff, Qs ≈ 0.

The Gash *et al*. (1995) model predicted rainfall interception loss:

$$\sum_{j=1}^{n+m} I_j = n(c)\,P'_G+(c\bar{E}_c/\bar{R})\sum_{j=1}^{n}(P'_{GJ}-P'_G)+(c)\sum_{j=1}^{m}P_{GJ}+qS_t+p_t\sum_{j=1}^{n-q}P_{GJ} \quad (6)$$

where, *I* is the interception loss depth, *m* is the number of small storms that is insufficient for saturating the canopy (*e.g.*, < P'_G), *n* equals the number of events which saturate the canopy (*e.g.*, > P'_G) and *q* equals the number of storms which saturate the trunks, P_{GJ} is gross rainfall, S_t is the trunk storage capacity, P_t is the proportion of rainfall reaching the trunks, and P'_G is amount of rainfall necessary to fill the canopy storage capacity (Eq. 7).

$$P'G=-\frac{\bar{R}Sc}{\bar{E}c}\ln\left[1-\frac{\bar{E}c}{\bar{R}}\right] \quad (7)$$

where: Ēc = the evaporation rate during the storm per unit area of cover, *Sc* = the canopy storage capacity per unit area of cover, $\bar{R}$ = the average rainfall rate onto the canopy.

The coefficient and parameter values used for this research are reported elsewhere (Návar-Cháidez and Lizárraga-Mendiola, 2013; Návar, 2013). E, is the soil water evaporated, Et, from the soil and water transpired by plants (Tr). Et, is usually weighted by E, θ, plant (Ftv), and climatic (Fc) factors. Soil factors that control Et are the current soil water content (θi), the soil water content at wilting point (θpmp), and the soil water content at field capacity (θcc). The plant factor is a function of vegetation, stocking, stand age, etc. Actual evapotranspiration is estimated using all these factors (Eq. 8):

$$Et=\frac{Ln\left[100*\frac{\theta_i-\theta_{pmp}}{\theta_{cc}-\theta_{pmp}}\right]}{Ln(101)}*E*Fc*Ftv \quad (8)$$

Soil physical parameters

Twelve soil samples were excavated within the watershed to estimate θcc, θpmp, soil bulk density (ρ_b) and soil specific density (ρ_c). The soil and litter layer depths were also measured.

Evaluating the time series for consistency

The SRWA was calculated by dividing the actual ring width value by the value predicted from the exponential decaying regression equation fitted to ring width over time (Fritts, 1976). The statistical parameters reflected the fact that the dendrochronologies have a high dendroclimatological potential. Annual SRWA data series were smoothed using a moving average of t=3; then, the autoregressive integrated moving average (ARIMA) models were fitted to this data set. The cumulative standardized z parameter for each hydro-climatic variable magnified oscillations or cycles.

Climate teleconnections

ENSO, PDO, and AMO control tree growth and are well described in reconstructed discharge and precipitation time series (Stahle *et al*., 1999; Cleaveland *et al*., 2003; Návar-Cháidez, 2012). The ENSO anomaly is defined by the difference between the Pacific Ocean surface temperatures and its average values. The accepted definition is a warming or cooling of at least 0.5°C, averaged over the east–central tropical Pacific Ocean. The ENSO has been divided into four major regions according to the location of temperatures in the Pacific Ocean. Four El Niño regions are reported as sea surface water temperatures, SST, or as sea surface temperature anomalies, SSTA, from reported means.

The SOI is the atmospheric component of El Niño

The SOI index has been recorded since 1948 and reconstructed since 1350. The warm PDO phase happens when the sea surface water of the Pacific Ocean coasts from Alaska to Baja California in Mexico is warmed and the cool phase reverts this pattern. The AMO has sea surface water temperatures measured from the equatorial Atlantic Ocean to the Greenland Coasts near the Arctic, covering the area from the African and European coasts in the east to the South and North American coasts to the west.

Associating tree growth and hydro-climatic variables

The ring width anomaly data for the dendrochronologies were associated with the hydro-climatic data derived

from the water balance model (1945-2007). The P, E, I, and Et, Q, and θ were available for a place in the upper ridges of the SMW, near El Salto, Durango, Mexico. ENSO was available in eight different forms; sea surface water temperatures and anomalies for all four El Niño regions: SST, SSTA, SST1, SSTA1, SST2, SSTA2, SST3, SSTA3, respectively. The data were available from weekly and monthly averages calculated from January of 1990 through March of 2012. The instrumental PDO data was available monthly from 1900 to 2012. The instrumental AMO data series was available annually from 1948 to 2012. The instrumental SOI index data series was available annually from 1948 to 2012. Reconstructed El Niño 3 (Cook, 2000), PDO (Biondi *et al*., 2001), AMO (Gray and Betancourt, 2004), SOI (Stahle *et al*., 1998), as well as P for Durango and Chihuahua (Stahle *et al*., 1999) were also available and related to the annual standard ring width anomaly for all three dendrochronologies as well.

Procedure

First, multiple regression equations in linear and non-linear fashions fitted the SRWA time series as the dependent variable with SST1, SSTA1, SST2, SSTA2, SST3, SSTA3, SST4, SSTA4, SOI, PDO, AMO, P, E, Et, Q, and θ as the independent variables from 1990-2001. Monthly hydro-climatic variable data were regressed against the SRWA index. Regression equations fitted different time-scale seasonal periods ($January_i$, $January_i$-$February_i$, $January_i$-$March_i$,….$January_i$-$September_i$). Using seasonal data from 1948 to 2001 (SOI, PDO, AMO, P, I, E, Et, Q, and θ), for example, for $November_{i-1}$-$December_{i-1}$, $November_{i-1}$-$January_i$,…, $November_{i-1}$-$September_i$, etc., a second set of equations correlated the effect of seasonal hydro-climatic variations on the SRWA. Third, using reconstructed data for PDO, AMO, SOI, and P for Durango and Chihuahua and the SRWA, a set of regression equations were developed for each dendrochronology. Finally, since the P, Et, and θ modeled by the mass balance approach explained a significant part of the SRWA anomaly, these variables were teleconnected with climatic events.

Results

Raw hydrologic, smoothed and modeled data using ARIMA techniques are depicted in Fig. 2 for the mean annual standard ring width anomaly.

Figure 3 depicts the magnification of cycles and oscillations using the monthly data series.

A larger ring width variability was observed in the past (1700's, 1750's, 1825's, 1850's) than in the present (2000's). The time series display the decadal drought episodes of the 1660's, 1690's, 1750's, 1800's, 1860's, 1930's, 1950's, and 1990's well (Figs. 2 and 3) because of a consistent reduction in the cumulative SRWA. Larger time-scale oscillations that ended and started somewhere in the early 1700-1750's, 1850's and 1960's are noted in the time series (Figs. 2 and 3). However, information is needed to more carefully check these potential cycles.

Associating variables of the hydrologic model with the standard ring width anomaly. Figure 4 shows the strength of the linear relationships between the SRWA and hydro-climatic variables as well as with climatic events (ENSO, SOI, PDO, and AMO), with statistically significant coefficients of determination (P=0.0001). Early in the season, January, the ENSO related events explained the most SRWA variability. As the season continued, the soil moisture content was the only variable that explained the SRWA variability for all three dendrochronologies. The statistical effect of the θ on the SRWA increased as the season continued and the strength of these relationships also increased. Evapotranspirations took over θ for the El Gato dendrochronology after May and also most Et in addition to climate synoptic events for Banderas after June (Fig. 4). For seasonal variables, θ was generally better related to the SRWA than the ENSO indices. However, in general, the SRWA variability was better explained statistically by the monthly hydro-climatic variables than by the seasonally related variables when using short-term data (Tab. 5, Fig. 4).

The hydro-climatic control of the standard ring width anomaly

A combination of the monthly ENSO indices and hydrological variables explained close to 90% of the total SRWA variability (Tab. 1).

For the Las Bayas dendrochronology, the ENSO, in addition to P, explained most of the SRWA variability. The maximum strength of this relationship was reached after March ($0.85 \leq r^2 \leq 0.92$) with a combination of ENSO, P, θ, and Et. For the El Gato chronology, only the ENSO parameters and P explained most of the SRWA variability. The strength of these relationships increased after May ($0.85 \leq r^2 \leq 0.89$). The Banderas SRWA was mostly described by P and ENSO and, here, the AMO control appeared to be an important source of SRWA variability as well. The strength of these relationships was largest after March ($0.93 \leq r^2 \leq 0.98$).

Longer time-scales (1948-2001)

The strength of the relationship between the SRWA and hydro-climatic variables declined for longer time series

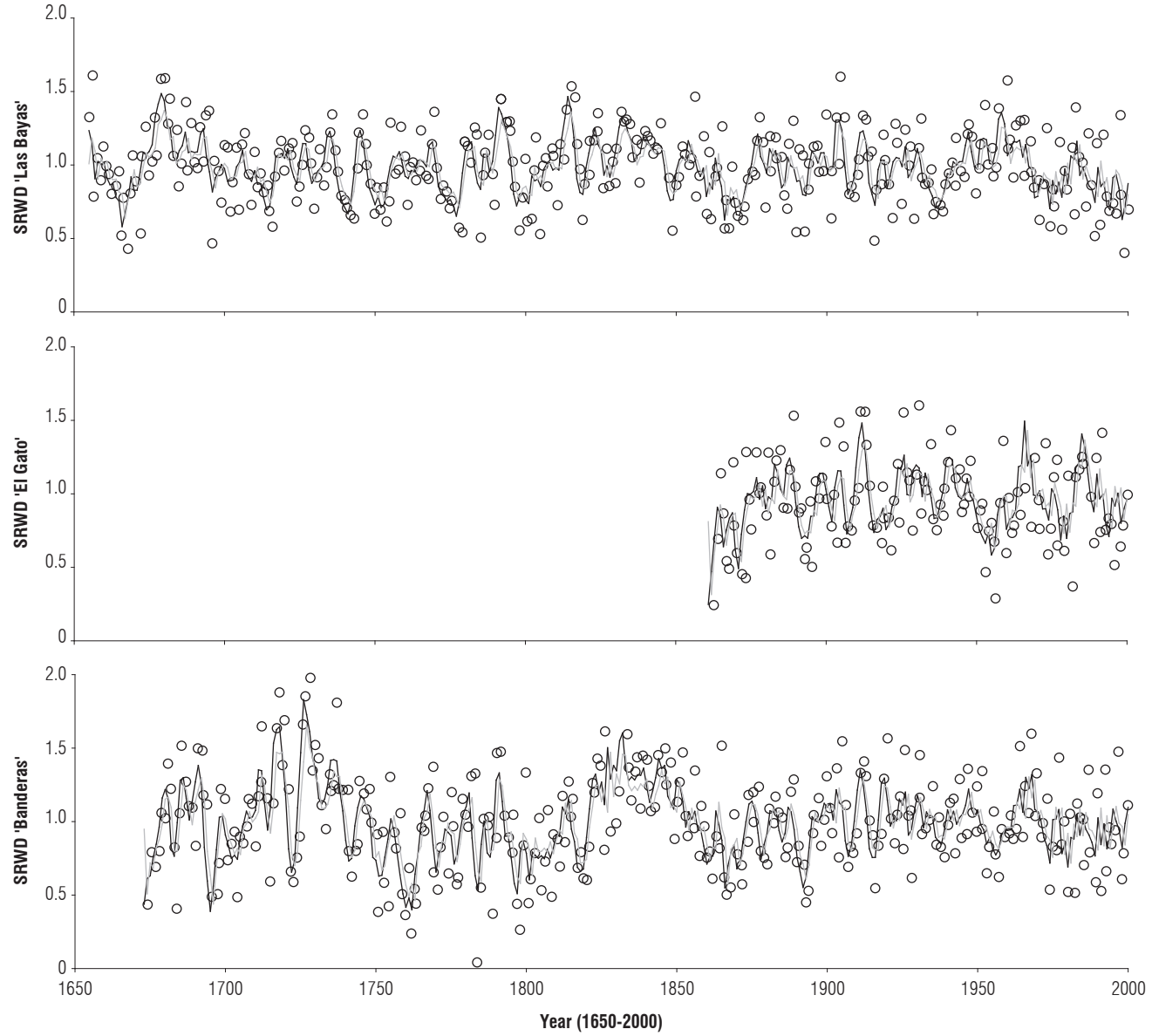

FIGURE 2. Standard ring width anomalies, SRWA, smoothed series, and ARIMA models for three time series (i) in Las Bayas, (ii) El Gato and (iii) Banderas of Durango, Mexico (note: black lines are smoothed raw data and gray lines are ARIMA models).

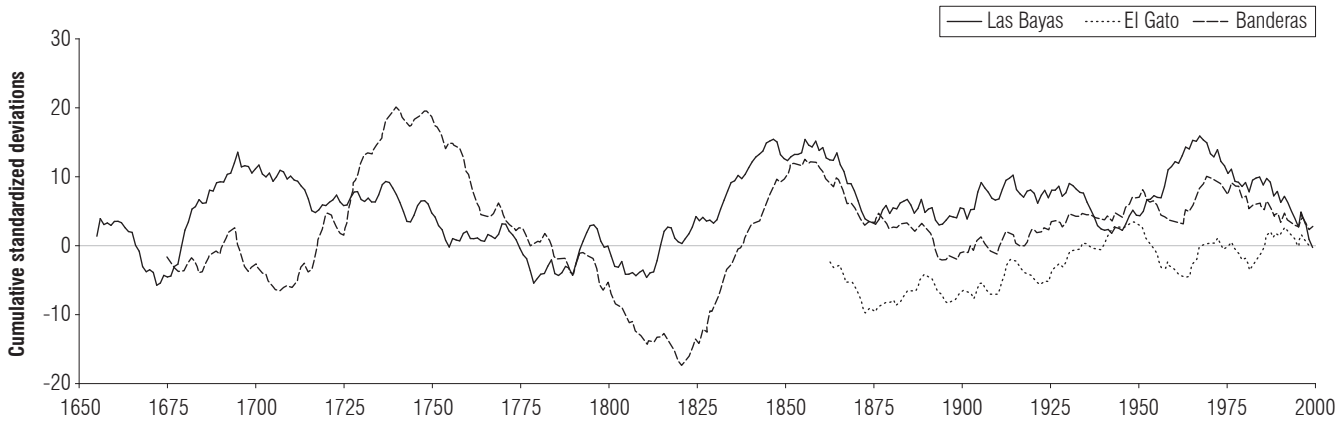

FIGURE 3. Cumulative standardized deviations of annual diameter growth for three northern Mexico dendrochronologies.

TABLE 1. Standard ring width anomaly variance explained by monthly hydro-climatic variability for three dendrochronolgies of Durango, Mexico (n =12: 1990-2001).

Month	Las Bayas (Durango)		El Gato (Zacatecas)		Banderas (Durango)	
	Variables	R^2	Variables	R^2	Variables	R^2
Jan	SST	0.35	SST1,P,SST3	0.73	P,AMO,SST3	0.77
Feb	SST1	0.36	SST1	0.41	θ	0.20
Mar	SST1,P,SST3,SOI,SST2	0.92	SST1,P,SST2	0.70	P,SST2,SST, θ	0.94
Apr	SST1,P,SST3	0.82	SST1,P,SST2	0.73	P,SST2,SST, θ	0.93
May	SST3,P,θ,Et	0.91	SST1,P,SST,SST3	0.89		
Jun	SST3,P, θ	0.86	SST1,P,SST,SST3	0.83		
July	SST3,P	0.85	SST1,P,SST2	0.81	P,SST2,SST,SOI,AMO	0.98
Aug	SST3,P	0.85	SST1,P,SST2	0.81	P,SST2,SST,SOI,AMO	0.98

Jan, January; Feb, February; Mar, March; Apr, April; Jun, June; Aug, August.

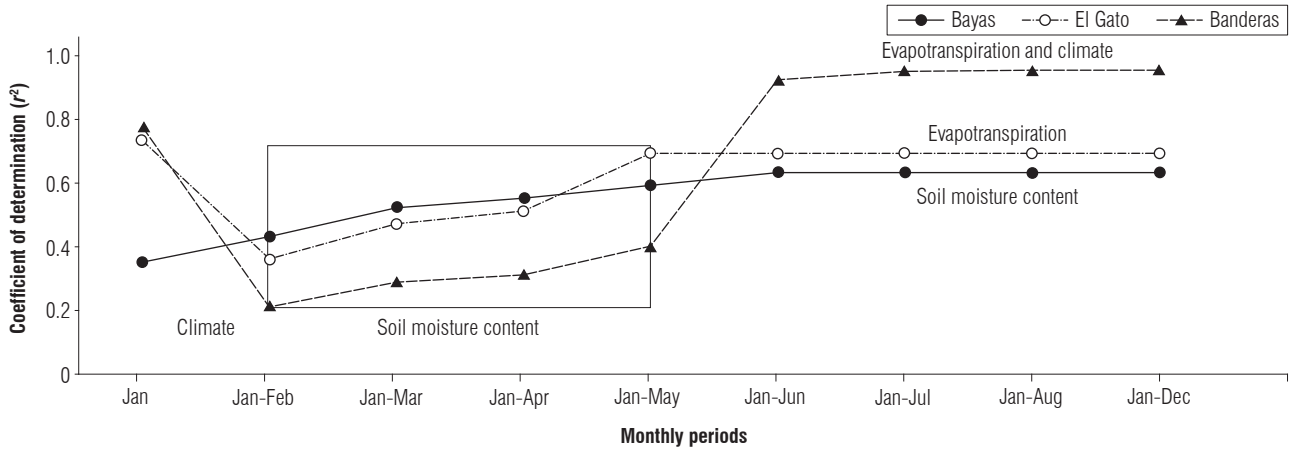

FIGURE 4. Strength of the relationship between the standard ring width anomaly and hydro-climatic variables for three dendrochronologies of the State of Durango, Mexico, for the period of 1990-2001 (n =12).

(Fig. 5). The November$_{i-1}$-June$_i$ period showed the largest r^2 between θ and SRWA for all three chronologies: Las Bayas (SRWA = -0.8837 + 5.5998θ; r^2=0.42); Banderas (SRWA = -0.9871 + 5.91θ; r^2 = 0.44); and the November$_{i-1}$-September$_i$ season for the El Gato chronology (SRWA = -2.453 + 9.39θ; r^2 = 0.49). In general, the single seasonal variable θ explained the most SRWA variability; $0.38 \leq r^2 \leq 0.49$. It accounted for more SRWA variability than seasonal P by 37% for all three chronologies. It also accounted for more SRWA variability than the large-scale synoptic events (SOI, PDO, AMO) by 57%. The forest and climate regulation effect on the soil water made the difference in this association. SOI, PDO, and AMO were again poorly linked to the SRWA variability (Fig. 5a).

Relating hydrological and climatic variables

Linear regression equations predicting θ, P, and Et as a function of climatic events produced intermediate coefficients of determination: θ = -0.1379 + 0.01946SST1, r^2 = 0.34, P=0.010; P=-4383.07 - 72.12SST + 257.86SST2, r^2 = 0.56, P=0.0021; Et = -1660.06 + 82.13SST2, r^2 = 0.41, P=0.0044. El Niño data positively explained θ and P. That is, high temperatures in the 3+4 El Niño region increased the regional P and Et values. The small θ variance explained by the model is probably due to the buffering effect of forest soils on all hydro-climate variables. The P variability was described by the sea surface temperatures of El Niño regions 1+2 and 3+4 and half of the remaining variation could not be explained by the other synoptic climate teleconnections, such as PDO or AMO.

Long-term relationships between hydro-climatic variables and the standard ring width anomaly

The equations showed that El Niño 3 and reconstructed P for Durango explained nearly 50% of the SRWA variability. The prediction equations are:

$$SRWA_{Las\ Bayas} = 0.56 + 0.037PDurango + 0.0053Niño3;$$
$$r^2 = 0.48;\ P=0.0001;\ n=320\ (1661\text{-}2001).$$

$$SRWA_{El\ Gato} = 0.59 + 0.119Niño3 + 0.0045PDurango;$$
$$r^2 = 0.42;\ P=0.0001;\ n=118\ (1863\text{-}2001).$$

$$SRWA_{Banderas} = 0.54 - 0.042PDO + 0.0058PDurango;$$
$$r^2 = 0.27;\ P=0.0001;\ n=306\ (1675\text{-}2001).$$

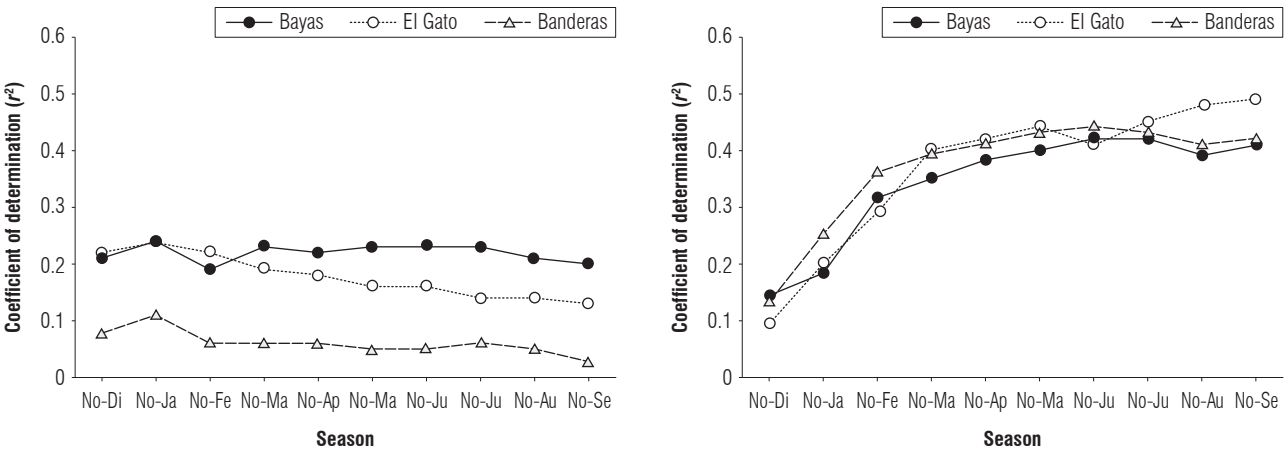

FIGURE 5. Strength of the relationship between: (a) the synoptic scale instrumental climatic variables (AMO, PDO, SOI) and the standard ring width anomaly and (b) the standard ring width anomaly and hydrological variables for three dendrochronologies of the State of Durango, Mexico for the period of 1948-2001 (n=215).

The tele-connection effect on the hydro-climatic variables

The SST in El Niño region 1 and its anomaly controlled the most P, E, Et, Q, and θ variability. The single equations associating the hydro-climatic variables and the large-scale synoptic events for the 4th lag time month are reported below.

$P_i = 2472 - 27.73AMO_{i-4} - 32.61SST_{i-4} + 25.20SSTA_{i-4} + 127.99SST1_{i-4} - 118.60SSTA1_{i-4}$; $r^2 = 0.63$; Sx = 54 mm; P=0.0001; n=215.

$E_i = -816 + 28.56SST1_{i-4} - 34.57SSTA1_{i-4} + 5.92SST2$; $r^2 = 0.90$; Sx = 9 mm; P=0.0001; n=215.

$Et_i = -1293 - 1837SST_{i-4} + 14.96SSTA_{i-4} + 68.29SST1_{i-4} - 63.55SSTA1_{i-4}$; $r^2 = 0.83$; Sx = 16 mm; P=0.0001; n=215.

$Q_i = -4.16 - 0.10AMO_{i-4} - 0.067SST_{i-4} + 0.045SSTA_{i-4} + 0.22SST1_{i-4} - 0.19SSTA1_{i-4}$; $r^2 = 0.33$; Sx = 0.16 mm; P=0.0001; n=215.

$\theta_i = -2.07 - 0.04SST_{i-4} + 0.034SSTA_{i-4} + 0.131SST1_{i-4} - 0.119SSTA1_{i-4}$; $r^2 = 0.61$; Sx = 0.05 cm cm^{-1}.

SST1 contributed the most to the P, E, Et, and Q variability and SST for θ. The second most important variable was SSTA1 for all variables and SST1 for θ. That is, El Niño region 2+3 appears to play a more significant role in local hydro-climatology than ENSO regions 3+4 or 4 or the AMO and PDO.

Discussion

Climate oscillations of different frequencies and time-scales regulated the SRWA anomaly. Pulses of different magnitudes and time intervals are the rule for the studied time series. For example, using the autocorrelograms and spectral density analysis, pulses of diameter growth were observed at several temporal scales: inter-annual, every 3-7 years; every 10-13 years and every 100-125 years.

The El Niño region 4 May precipitation, May θ, and May Et explained 91% of the total SRWA variability for the Las Bayas dendrochronology. For the El Gato dendrochronology, El Niño region 3, May P, and the El Niño regions 1+2 and 4 explained close to 90% of the total SRWA variability. March P and θ and El Niño 3+4 and 1+2 explained 94% of the total SRWA variability for the Banderas dendrochronology. This erratic pattern of the hydro-climatic variables associated with diameter growth between the dendrochronologies of *P. menziesii* has been attributed to potential localized hydro-climatic variations within the Sierra Madre Occidental mountain range. Las Bayas is located in the upper ridges of this mountain range near the continental and climatic divide, while El Gato and Banderas are found at the leeward side of the SMW, neighboring the Central Valleys of Durango and Chihuahua. Banderas is found north (*c.a.* 500 km) of El Gato; a large spatial difference in a region dominated by a monsoonal climate and controlled by local aspect and topography (Comrie and Glenn, 1998). Návar (2014) predicted, with geographical equations, that the leeward side of the northwestern SMW is the wettest of Durango's interior basins, while the upper windward ridges of the southwestern portion of the Sierra Madre Occidental mountain range is the wettest of the Pacific Ocean watersheds. Tree ring width data has also been mostly associated with ENSO indices in Durango, Mexico (Cleaveland *et al*., 2003). The PDO was related to ring width anomalies for Alaskan trees (D'Arrigo *et al*., 2006).

Precipitation is the single most important variable associated with the diameter growth of *P. menziesii* for the Banderas dendrochronology and the second most important for Las Bayas and El Gato; as supported by numerous other related studies (González-Elizondo *et al*., 2005; Therrell *et al*., 2006; Arreola-Ortiz and Návar-Cháidez, 2010). However, the most diameter growth variation explained by precipitation hardly surpassed 50% of the total variability. Although the ENSO climatic event is more related to diameter growth than to PDO or AMO, its effect is inconsistent since several El Niño regions are associated differently to this variable. El Niño events are characterized by cold and wet winters (Cavazos and Hastenrath, 1990; Návar-Cháidez, 2011) and provide the most suitable conditions for pine tree growth in northern Mexico because of its holartic origin (Cleaveland *et al*., 2003; González-Elizondo *et al*., 2005). The PDO has been associated with the diameter growth of white spruce trees in Alaska (D'Arrigo *et al*., 2006). The AMO appears as a significant variable for the chronology of Banderas but its explanation power is weak. The length of the synoptic scale climate variability time series may be problematic for associating AMO and PDO with ring width anomalies since these last two climatic phenomena appear on time scales of more than 20 years.

Seasonal θ explains the most diameter growth variability of *P. menziesii* trees of Durango, Mexico for both temporal scales (1990-2001 and 1948-2001). For the first time series (1990-2001), the relationship between θ and SRWA was stronger ($0.21 \leq r^2 \leq 0.63$) than for the second one ($0.18 \leq r^2 \leq 0.49$). As the time series increases over time the power prediction diminishes, stressing the importance of other variables that play significant roles in diameter growth as well. This finding has a physiological interpretation as trees require soil water early in the growth season (February and/or March) to fully display diameter growth. The strength of this relationship increases as the season continues, attaining a steady value of 63, 51, and 40% of the total SRWA variability for the dendrochronologies of Las Bayas, El Gato, and Banderas, respectively. The seasonal θ for January-June, January-April, and January-May record these variabilities well. For El Gato and Banderas, seasonal Et took over θ after June, explaining close to 70% of the total SRWA variability. So, cold wet winters followed by warm-wet summers with high actual evapotranspiration rates are the most suitable conditions for tree diameter growth. The physiological interpretation of the role Et plays in diameter growth also has a physical meaning since trees capture more CO_2 by opening the stomata and losing water vapor to the atmosphere during this process.

This research shows how difficult it is to associate climatic variability with diameter growth in forests since soils partially buffer this effect. The simple explanation for this finding demonstrates the best relationship seen between θ and SRWA rather than by any other source of climatic variability, such as ENSO, PDO, or AMO. The soil variables that may be important in explaining this variability are: soil depth, soil porosity, field capacity and wilting point. These physical parameters must explain an important part of the diameter variability left by soil moisture content itself. Other variables explaining diameter variability that may change over time are: tree competition; or competition between trees, soil fertility status, and frosts, among others.

Conclusions

Climate was teleconnected to the diameter growth of *P. menziesii* and four months is the lag time required for the El Niño Southern Oscillation to display its effect on diameter growth. The forest soil partially buffered the hydro-climatic effect and, therefore, the soil moisture content was better related to the standard ring width anomaly than the large-scale synoptic climatic events themselves. Future research must center on how soil drought spells control tree growth.

Literature cited

Arreola-Ortiz, M.R. and J.J. Návar-Cháidez. 2010. Análisis de sequías y productividad con cronologías de *Pseudotsuga menziesii* Rob. & Fern., y su asociación con EL Niño en el nordeste de México. Invest. Geog. 71, 7-20.

Biondi, F.L., A. Gershunov, and D.R. Cayan. 2001. North Pacific decadal climate variability since 1661. J. Climate 14, 5-10.

Briffa, K. 2000. Annual climate variability in the Holocene: interpreting the message of ancient trees. Quaternary Sci. Rev. 19, 87-105.

Cavazos, T. and S. Hastenrath. 1990. Convection and rainfall over Mexico and their modulation by the Southern Oscillation. Int. J. Climatol. 10, 377-386.

Cleaveland, M.K., D.W. Stahle, M.D. Therrell, J. Villanueva-Diaz, and B.T. Burns. 2003. Tree-ring reconstructed winter precipitation and tropical teleconnections in Durango, Mexico. Climate Change 59, 369-388.

Comrie, A.C. and E.C. Glenn. 1998. Principal components-based regionalization of precipitation regimes across the southwest United State and northern Mexico, with application to monsoon precipitation variability. Climate Res. 10, 201-215.

Cook, E.R. 2000. Niño 3 index reconstruction, unpublished data. In: National Climatic Data Center/National Oceanic and Atmospheric Administration (NOAA), http://www.ncdc.noaa.gov/data-access/paleoclimatology-data/datasets/climate-reconstruction; consulted: February, 2014.

Cook, E., J.S. Glitzenstein, P.J. Krusic, and P.A. Harcombe. 2001. Identifying functional groups of trees in west Gulf Coast Forests (USA): a tree ring approach. Ecol. Appl. 11, 883-903.

D'Arrigo, R., E. Mashing, D. Frank, and G. Jacoby. 2006. North Pacific-related climate variability inferred from seaward Peninsula, Alaska tree rings since A.D. 1358. Climate Dyn. 24, 227-236.

Dueñez-Alanís, J., J. Gutiérrez, L. Pérez, and J. Návar. 2006. Manejo silvícola, capacidad de infiltración, escurrimiento superficial y erosión. Terra Latinoam. 24, 233-240.

Enfield, D.B., A.M. Mestas-Nunez, and P.J. Trimble. 2001. The Atlantic multidecadal oscillation and its relation to rainfall and river flows in the continental U.S. Geophys. Res. Lett. 28, 2077-2080.

Fang, K., X. Gou, F. Chen, E. Cook, J. Li, and Y. Li. 2012. Spatiotemporal variability of tree growth and its association with climate over Northwest China. Trees 26(5), 1471-1481.

Fritts, H.C. 1976. Tree rings and climate. Academic Press, London.

García, E. 1987. Modificaciones al sistema de clasificación climática de Köppen (adaptación a la Republica Mexicana). 4th ed. Universidad Nacional Autónoma de México (UNAM), Mexico DF.

Gash, J.H.C., C.R. Lloyd, and G. Lachaud. 1995. Estimating sparse forest rainfall interception with an analytical model. J. Hydrol. 170, 79-86.

González-Elizondo, M., E. Jurado, J. Návar, M.S. González-Elizondo, J. Villanueva, O. Aguirre, and J. Jiménez. 2005. Tree-rings and climate relationships for Douglas-fir chronologies from the Sierra Madre Occidental, México: a 1681-2001 rain reconstruction. Forest Ecol. Manag. 213, 39-53.

Gray, S. and J. Betancourt. 2004. Atlantic multidecadal oscillation index reconstruction. In: National Climatic Data Center/National Oceanic and Atmospheric Administration (NOAA), ftp://ftp.ncdc.noaa.gov/pub/data/paleo/treering/reconstructions/amo-gray2004.txt; consulted: February, 2014.

Jones, D.L. 2003. El Niño, PDO, climatic cycles and drought in the Sierra Nevada. El Dorado County Water Agency; Water Resources Development and Management Plan, San Diego, CA.

Knight, J.R., C.K. Folland, and A.A. Scaife. 2006. Climate impacts of the Atlantic Multidecadal Oscillation. Geophys. Res. Lett. 33(17), LI7706.

Linderholm, H.W., B.O. Solberg, and M. Lindholm. 2003. Tree-ring records from central Fennoscandia: the relationship between tree growth and climate along a west-east transect. The Holocene 13(6), 887-895.

Mantua, N.J., S.R. Hare, Y. Zhang, J.M. Wallace, and R.C. Francis. 1997. A Pacific Interdecadal Climate Oscillation with impacts on salmon production. Bull. Amer. Meteor. Soc. 78(6), 1069-1079.

Návar, J. 2008. Atlas hidrológico del estado de Durango. Instituto Politecnico Nacional, Durango, Mexico.

Návar, J. 2013. The performance of the reformulated Gash's interception loss model in Mexico's northeastern températe forests. Hydrol. Proc. 27, 1626-1633.

Návar, J. 2014. Spatial and temporal hydro-climatic variability in Durango, Mexico. Tecnol. Cienc. Agua 1(1), 103-123.

Návar-Cháidez, J.J. 2011. Modelación del contenido del agua de los suelos y su relación con los incendios forestales en la Sierra Madre Occidental de Durango, México. Madera y Bosques 17(3), 65-81.

Návar-Cháidez, J.J. 2012. Modeling annual discharge for six Mexico's northern subtropical rivers. Rev. Ambient. Agua 7, 36-50.

Návar-Cháidez, J.J. and L.G. Lizárraga-Mendiola. 2013. Hydroclimatic variability and forest fires in Mexico's northern temperate forests. Geofís. Int. 52, 5-20.

Sheppard, P.R., A.C. Comrie, G.D. Packin, K. Angersbach, and M.K. Hughes. 2002. The climate of the US Southwest. Climate Res. 21, 219-238.

Stahle, D.W., R.D. D'Arrigo, P.J. Krusic, M.K. Cleaveland, E.R. Cook, R.J. Allan, J.E. Cole, R.B. Dunbar, M.D. Therrell, D.A. Gay, M.D. Moore, M.A. Stokes, B.T. Burns, J. Villanueva-Diaz, and L.G. Thompson. 1998. Southern oscillation index reconstruction. In: National Climatic Data Center/National Oceanic and Atmospheric Administration (NOAA), ftp://ftp.ncdc.noaa.gov/pub/data/paleo/treering/reconstructions/soi_recon.txt; consulted: February, 2014.

Stahle, D.W., M.K. Cleaveland, M.D. Therrell, and J. Villanueva-Diaz. 1999. Tree ring reconstruction of winter and summer precipitation in Durango, Mexico, for the past 600 years. pp. 205-211. In: Proc. 10th Symposium Global Change Studies. Amer. Meteor. Soc., Boston, MA.

Swetnam, T.W. and J.L. BetancourtJ. 1998. Mesoscale disturbance and ecological response to Decadal Climate Variability in the America Southwest. J. Climate 11, 3128-3147.

Therrell, M.D., D.W. Stahle, J. Villanueva-Diaz, E. Cornejo-Oviedo, and M. Cleaveland. 2006. Tree-ring reconstructed maize yield in Central Mexico: 1474-2001. Climate Change 74, 493-504.

Tingstad, A.H., and G.M. MacDonald. 2010. Long-term relationships between ocean variability and water resources in northeastern Utah. J. Amer. Water Resour. Assoc. 46(5), 987-1002.

Valente, F., J.S. David, and J.H.C. Gash. 1997. Modelling interception loss for two sparse eucalypt and pine forests in central Portugal using reformulated Rutter and Gash analytical models. J. Hydrol. 190, 141-162.

Worbes, M. 2002. Annual growth rings, rainfall-dependent growth and long-term growth patterns of tropical trees from the Caparo Forest Reserve in Venezuela. J. Ecol. 87, 391-403.